EVALUATION OF THE SWARM MVMO FOR PHOTOVOLTAIC PARAMETER ESTIMATION IN A DOUBLE-DIODE MODEL

Gustavo Henrique de Paula Santos – gustavohenrique@ifsp.edu.br
Instituto Federal de Educação, Ciência e Tecnologia de São Paulo, Campus Campinas
Elmer Pablo Tito Cari
Universidade de São Paulo, Escola de Engenharia de São Carlos, Departamento de Engenharia Elétrica e Computação

Abstract. *Photovoltaic energy is expanding due to its generation performance, cost, and useful life. In this sense, it is essential to develop models and techniques that can improve the efficiency of systems. Analytical, metaheuristic, and hybrid methods have been used to estimate the parameters of Single-Diode Model (SDM) and Double-Diode Model (DDM), but none solve all the problems, thus requiring the development of new techniques. In this work, the Swarm MVMO method was used to estimate the parameters of the double diode model using data from the photovoltaic cell RTC France. The results obtained show that Swarm MVMO was effective, reaching the same level of RMSE as other algorithms in the literature and achieving a good fit in the I-V and P-V curves.*

Keywords: *Swarm MVMO; Parameter Estimation of Photovoltaic Systems, Double-diode model (DDM).*

1. INTRODUCTION

Photovoltaic energy has an impact on generation and is increasing significantly. Its attractiveness is mainly due to its generation performance, cost, and useful life. During its useful life, the photovoltaic system is exposed to various environmental conditions that can result in a gradual decrease in performance, failures, and loss of power (Aghaei et al., 2022). In this sense, the development of photovoltaic models allows the control, optimization, and prediction of energy, which constitute essential tools for the integration of systems into the grid (Elhammoudy et al., 2023). Some research has been conducted in an attempt to enhance photovoltaic efficiency, with particular emphasis placed on the estimation of photovoltaic model parameters. Adjusted parameters have the potential to enhance system performance, rendering this topic notably pertinent (Yu et al., 2022).

The mathematical models of the single-diode model (SDM) and double-diode model (DDM) are the most used to define a solar cell (Oliva et al., 2017) (Ramadan et al., 2022). SDM is the most used in studies due to its simplicity and precision, however, DDM provides greater precision at higher levels of solar irradiance by including the recombination losses that occur in the depletion zone (Ridha et al., 2022). Examples of the application of the models can be seen in Ćalasan, Aleem, and Zobaa (2021) and Sharadga, Hajimirza and Cari (2021).

In the literature, the three main methods applied to estimating photovoltaic parameters are listed: analytical, metaheuristic, and hybrid as can be seen in Elkholy and Abou (2019), Nguyen et al. (2022), Gao et al. (2021), respectively. Analytical methods are based on the derivation of mathematical equations that provide a simple and quick way to identify and calculate photovoltaic parameters (Diab et al., 2020). Meta-heuristic methods convert the photovoltaic module parameter estimation problem into an optimization problem due to their non-linear, limited, and continuous characteristics (Saadaoui et al., 2021). Hybrid methods were developed due to the limitations of metaheuristics. These methods can achieve greater accuracy as they combine the best of both methods, but there is greater computational effort and implementation difficulty (Ridha et al., 2021).

Although optimization techniques have been researched and tried in the literature, none solve all problem types. New optimization techniques must be employed to evaluate performance in different benchmark function types (Premkumar et al., 2021). Despite the meta-heuristic algorithms obtaining sufficiently satisfied results in parameter estimation of PV models, no algorithm is perfect (Long et al., 2022). In this regard, the mathematical modeling of PV systems and the estimation of model parameters with appropriate optimization algorithms is still an existing challenge and continues at a greater pace (Demirtas and Koc, 2022). This research proposes the Swarm Mean-Variance Mapping Optimization algorithm (Swarm MVMO) to estimate the parameters of a PV cell with literature-reported data using DDM. The Swarm MVMO is a type of evolutionary algorithm that focuses on optimizing a single solution, in contrast to other evolutionary algorithms that work with a group of solutions (Shouman, Hegazy, and Omran, 2021).

2. PHOTOVOLTAIC MODEL

The basic photovoltaic model, SDM, has 5 unknown parameters that must be determined for an adequate representation of the I -V characteristics, however, this model does not represent all physical aspects. Its equivalent electrical circuit is composed of a direct current source (I_{ph}), a diode (D_1), a resistance in parallel (R_{sh}), and another in

series (R_s). The current flowing through the diode can be represented by two parameters: the ideality factor (a_1) and reverse saturation current (I_{s1}) (Ćalasan, Aleem, and Zobaa, 2021). DDM, shown in Fig. 1, is based on SDM where only a second diode is added in parallel with the current source to investigate the recombination loss of the space charge regions of the $p - n$ junction (Nguyen, Nguyen, and Tran, 2022). Diode D_1 simulates the minority carrier diffusion process in the depletion layer, while D_2 represents carrier recombination in the space charge region of the junction (Gao et al., 2016). The DDM has 7 unknown parameters: I_{ph}, I_{s1}, I_{s2}, a_1, a_2, R_s, and R_{sh}.

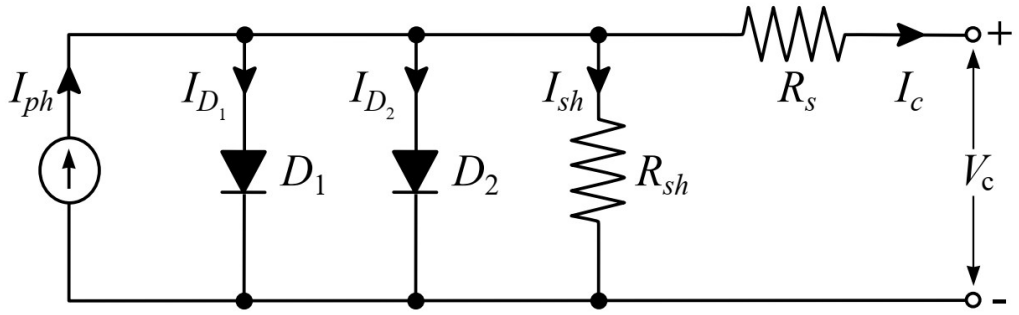

Figure 1- DDM electric circuit (Nguyen, Nguyen, and Tran, 2022).

Applying Kirchhoff's current law on the circuit of Fig. 1, the cell output current (I_c) is given by solving the implicit Eq. 1, where I_{sh} is the shunt resistor current. The diode currents I_{D1} and I_{D2} represent diffusion and recombination currents expressed by the Shockley equation according to Eqs. 2 and 3.

$$I_{ph} - I_{D_1} - I_{D_2} - I_{sh} - I_c = 0 \tag{1}$$

$$I_{D_1} = I_{s1}\left\{exp\left[\frac{q(V_c + R_s I_c)}{a_1 k T_c}\right] - 1\right\} \tag{2}$$

$$I_{D_2} = I_{s2}\left\{exp\left[\frac{q(V_c + R_s I_c)}{a_2 k T_c}\right] - 1\right\} \tag{3}$$

where I_{s1} and I_{s2} are the diode reverse saturation current of diodes D_1 and D_2 respectively, q is the electron charge ($1.60217646 \times 10^{-19}$ C), V_c is the cell output voltage, a_1 and a_2 are the diode ideality factor of diodes D_1 and D_2 respectively, k is the Boltzmann constant ($1.3806503 \times 10^{-23}$ J/K), and T_c is the cell temperature (K). Finally, the shunt resistor current is given by Eq. 4.

$$I_{sh} = \frac{V_c + R_s I_c}{R_{sh}} \tag{4}$$

3. SWARM MEAN-VARIANCE MAPPING OPTIMIZATION (SWARM MVMO)

MVMO is a population-based stochastic optimization technique. Its similarity with differential evolution algorithms, genetic algorithms, and particle swarm optimization which uses the ideas of selection, mutation, and crossover, however, as the main characteristic of the MVMO method, the transformation of mutated genes is based on the mean and variance of the best individuals in the population (Erlich, Venayagamoorthy, and Worawat, 2010). To improve the global search capability, the swarm concept is incorporated into the MVMO method (Swarm MVMO). This way, multiple particles will be part of the estimation process. Particles are made up of individuals and individuals are made up of genes (Rueda and Erlich, 2013a and Rueda and Erlich, 2013b).

The method begins in the setup step where the algorithm parameters are configured and random samples of optimization variables are generated within their specified search limits for a total number of particles (*NP*) (candidate solutions) and stored in a solution archive. Then, the optimization variables are normalized, transforming the search space for all variables into the range between 0 and 1. This normalization is a prerequisite for the mutation operation through the mapping function and ensures that the generated descendants do not violate search limits. Finally, the optimization variables are denormalized again before the fitness evaluation or local search processes are executed. At each evaluation, the solution file is updated based on whether the particles are classified as good or bad and the process ends when the termination criterion is satisfied (Rueda and Erlich, 2013b). Fig. 2 shows the Swarm MVMO flowchart where i is the function evaluation counter, c is the particle counter, m is the number of particles, and i_{max} is the maximum number of fitness function evaluations.

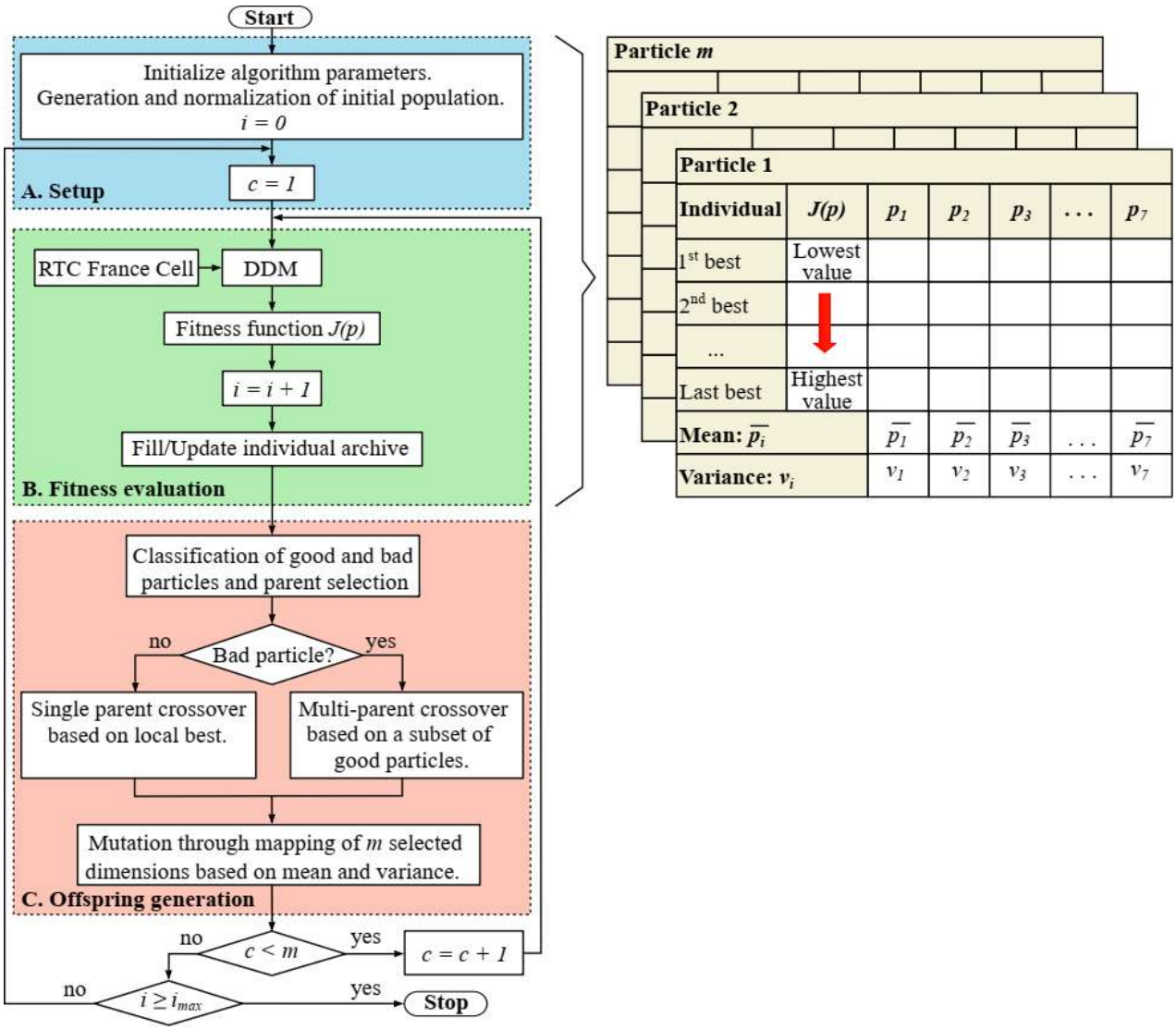

Figure 2- Swarm MVMO flowchart including the solution archive with all *NP* particles (adapted from Rueda and Erlich, 2013b).

In the fitness evaluation phase, the measurement data obtained from the photovoltaic system is applied to the photovoltaic model considering each individual of the particles generated in the previous step and the results are evaluated in the fitness function described in Eq. 5 (based on the Root Mean Square Error - RMSE). Then, according to the results of the fitness function, individuals are ranked from the lowest to the highest value of the fitness function in each particle.

$$J(p) = \sqrt{\frac{1}{M}\sum_{j=1}^{M} f(u, y, p)^2} \tag{5}$$

where p is the estimated parameter vector Eq. 6, M is the number of samples of measurement data, u is the input vector of the model according to Eq. 7, y is the output vector of the model according to Eq. 8, and $f(u, y, p)$ is the implicit model function of DDM described by Eq. 9.

$$p = [I_{ph}, I_{s1}, I_{s2}, a_1, a_2, R_s, R_{sh}] \tag{6}$$

$$u = [V_c(t), T_c] \tag{7}$$

$$y = [I_c(t)] \tag{8}$$

$$f(u,y,p) = I_{ph} - I_{s1}\left\{exp\left[\frac{q(V_c + R_s I_c)}{a_1 k T_c}\right] - 1\right\} - I_{s2}\left\{exp\left[\frac{q(V_c + R_s I_c)}{a_2 k T_c}\right] - 1\right\} - \frac{V_c + R_s I_c}{R_{sh}} - I_c \tag{9}$$

The individual of each particle that presents the lowest value of the fitness function is classified as the local best. Particles are classified by their respective local best individuals, from lowest value to highest value. The particle containing the local best individual with the lowest value of fitness function is classified as the global best. Two groups are formed according to the particle classification: the good particles (GP) and the bad particles (BP). These groups are based on the multi-parent strategy of the offspring stage for the next generation. Equations 10 and 11 present the father for the GP and BP groups, respectively. Fig. 3 shows the offspring creation of bad particles according to Eq. 11 including the mutation process by mapping function with local mean and variance.

$$x_p^{parent} = x_i \tag{10}$$

$$x_p^{parent} = x_k + \beta(x_i - x_j) \tag{11}$$

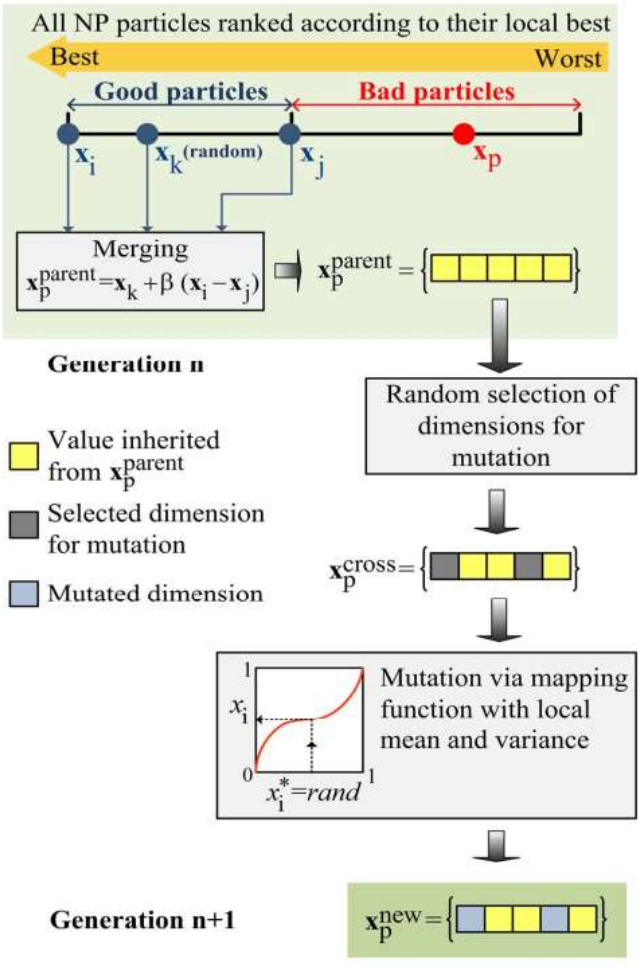

Figure 3 - Offspring generation stage for BP (Rueda and Erlich, 2013[2]).

where x_p^{parent} is the father of GP or BP, X_i is the global best in the GP group, X_j is the last particle of the GP group, X_k is a random particle in the GP group, and β is a random number between 0 to 1 to re-draw the elements. In the crossover step, a random number of genes (in this work each gene refers to a DDM parameter) is chosen for mutation originating X_p^{cross}. The strategy of this stage is based on roulette wheel tournament selection. Finally, in the mutation step, the

chosen genes, are submitted to the mapping function. The new individual is determined by Eq. 12, where x_p^* is a random number between 0 to 1 and h represents the mapping function described by Eq. 13 with h_p, h_1, and h_0 as the outputs of the mapping function, according to Eq. 14. The shape factor calculated by Eq. 15 is based on variance, where f_s is the scaling factor. More information about MVMO can be found in Erlich, Venayagamoorthy, and Worawat, (2010).

$$x_p^{new} = h_p + (1 - h_1 + h_0)x_p^* - h_0 \tag{12}$$

$$h(\bar{x}, s_1, s_2, x) = \bar{x}(1 - e^{-xs_1}) + (1 - \bar{x})e^{-(1-x)s_2} \tag{13}$$

$$h_p = h\left(x = x_p^*\right), \qquad h_0 = h(x = 0), \qquad h_1 = h(x = 1) \tag{14}$$

$$s_{1\ or\ 2} = -\ln(v_i)f_s \tag{15}$$

The factors s_1, s_2, and $\bar{x}$ define the format of the mapping function curve. The graph of Fig. 4a displays the influence of $\bar{x}$ on the mapping function curve plotted for individuals' values of 0, 0.25, 0.5, 0.75, and 1. In the graph of Fig. 4b, $\bar{x}$ is fixed in 0.5 (mean between 0 to 1) to display the influence of s_1 and s_2 when they have the same values ($s_1 = s_2$). The decrease in variance given by Eq. 15 increases the shape factor and makes the mapping function curve flatter, so the space to be searched is focused on the region near to mean value. In this graph, the mapping function curve is plotted for shape factor values of 0, 5, 10, 15, and 50. On the one hand for the shape factor equal to 0, every value assigned to x_p^* (random) will generate a different value of x_p. On the other hand, for a shape factor equal to 50, any value assigned to x_p^* (random) will generate a value close to the mean of x_p. Fig. 4c and 4d show the influence of s_1 and s_2 when they have different values, which makes the curve of the mapping function asymmetric.

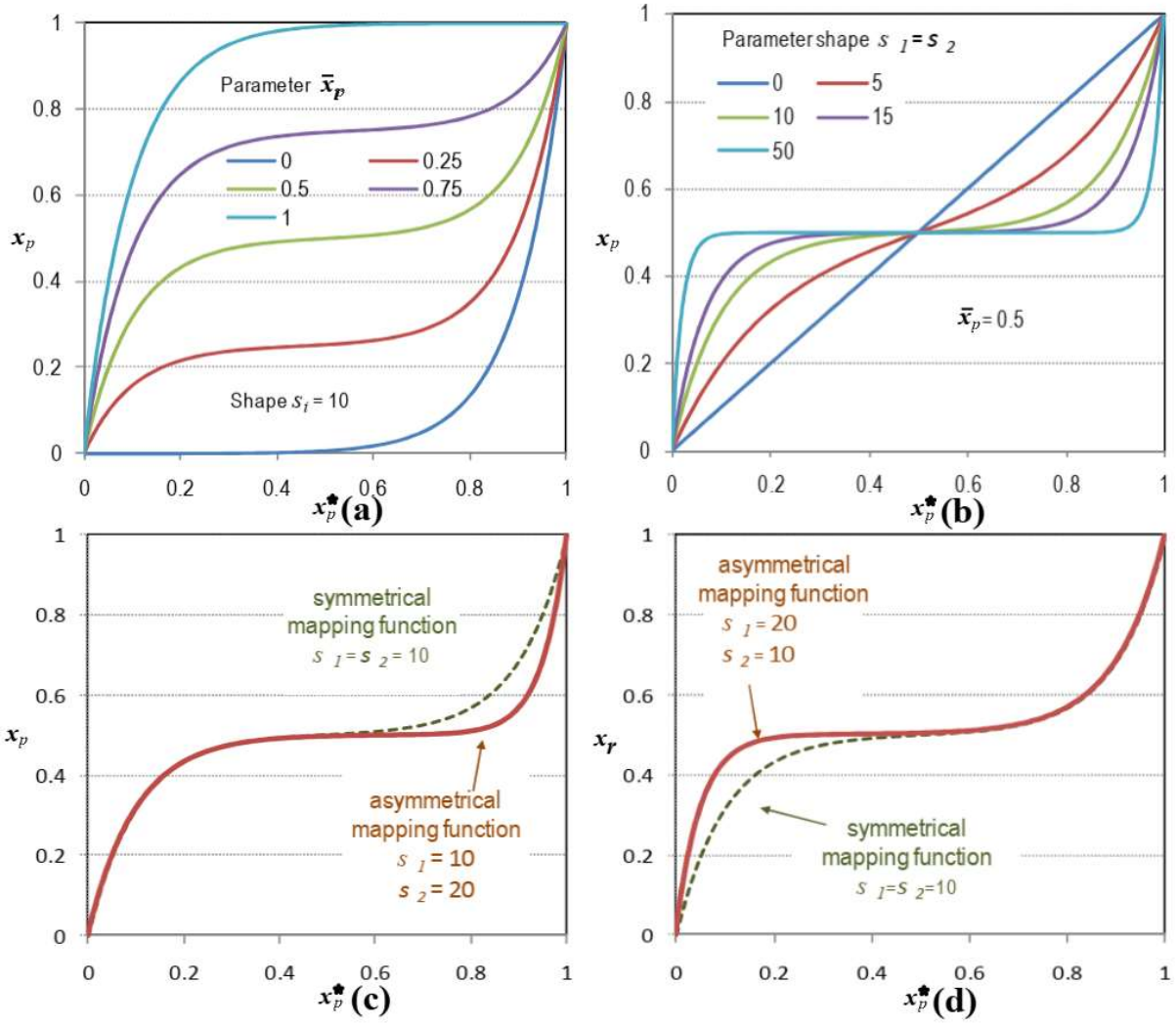

Figure 4 – Mapping function: influence of mean and variance (Erlich, Venayagamoorthy, and Worawat, 2010).

4. RESULTS AND DISCUSSION

The performance of Swarm MVMO for PV parameter estimation of DDM is conducted using the PV dataset widely studied in the literature as can be seen in Yaghoubi et al. (2022), Ramadan, Khan, and Diab (2022), Huynh, Dunnigan, and Barbalata (2022), and Demirtas and Koc, (2022). This dataset contains the I - V measurement from an RTC France silicon solar cell with a diameter of 57 mm obtained in Easwarakhanthan et al. (1986) under G = 1000 W/m^2 and T = 33º C. The settings of Swarm MVMO, described in Tab. 1, are based on Erlich, Venayagamoorthy, and Worawat, (2010), Rueda and Erlich, (2013a), and Rueda and Erlich, (2013b). The search limits of each parameter, also described in Tab. 1, are based on Yaghoubi et al. (2022) and Bo et al., (2022). Matlab R2022b using an 11th Gen Intel® Core™ i5-11400 @ 2.60 GHz 2.59 GHz, 24 GB RAM with Windows(R) 11, 64 bits was used for the simulations.

Table 1 – Setup of Swarm MVMO.

Description		Value
Number of parameters to be estimated (p_n)		7
Number of individuals per particle (X_n)		5
Maximum number of fitness evaluations (i_{max})		50000
Number of particles (m)		105
Simulations number (runs)		30
Search limits (Lower and upper bounds)	I_{ph} (A)	0 – 1
	I_{s1} (µA)	0 – 1
	I_{s2} (µA)	0 – 1
	a_1 (-)	1 – 2
	a_2 (-)	1 – 2
	R_s (Ω)	0 – 0.5
	R_{sh} (Ω)	0 – 100

The lower RMSE value of the 30 runs was 0.986E−03 which estimated the best PV parameters. The highest RMSE value was 1.422439E−03, the average value was 1.113071E−03 and the STD was 1.092937E−04. Fig. 5 shows the RMSE values of each run and the average time for one run was 146 seconds.

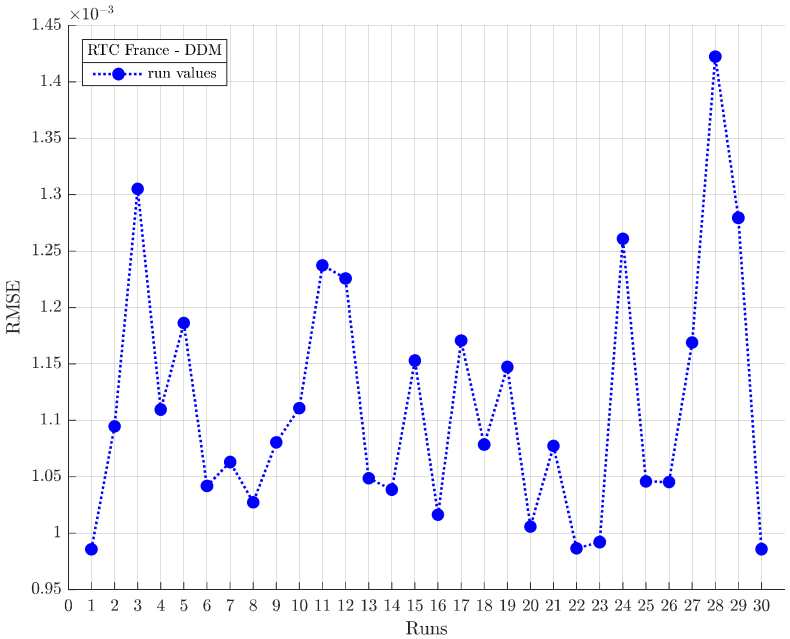

Figure 5 – RMSE values per run.

Table 2 shows the best-estimated parameter values and their corresponding values in the literature references for comparison purposes. Swarm MVMO reached the same levels of the RMSE values from the literature. The estimated value for the I_{ph}, R_s, and R_{sh} parameters varied the least compared to other algorithms in the literature, however, the parameter values of I_{s1}, I_{s2}, a_1, and a_2 did not maintain this uniformity. The I - V and P - V curves with the best parameters are shown in Figs. 6 and 7, where the measured values and the estimated values are found in a good fit. The dataset with V_{mea}, I_{mea}, I_{est}, I_{ae}, P_{mea}, and P_{est} are related in Tab. 3 where can be seen the low value of the sum of the absolute error and the RMSE of current and power.

Table 2 – Estimated parameters and literature reference values from other algorithms.

Algorithm	I_{ph} (A)	I_{s1} (μA)	I_{s2} (μA)	a_1 (-)	a_2 (-)	R_s (Ω)	R_{sh} (Ω)	RMSE
Swarm MVMO	**0.7608**	**0.3079**	**0.0574**	**1.4773**	**1.8521**	**0.0364**	**53.9285**	**0.986E-03**
MSSA	0.7608	0.9731	0.1679	1.9213	1.4281	0.0369	53.8368	0.983E-03
RN-ChOA	0.7608	0.2228	0.7272	1.4512	2.0000	0.0364	55.4264	0.972E-03
QRMSCS	0.7608	0.2260	0.0749	1.4510	2.0000	0.0367	55.4854	0.982E-03
CJAYA4	0.7607	0.3030	0.3160	1.4769	1.9965	0.0362	57.0983	0.983E-03
INFO	0.7608	0.7493	0.2260	2.000	1.4510	0.0367	55.4854	0.982E-03

Note: Modified Salp Swarm Algorithm (MSSA) from Yaghoubi et al. (2022). Robust Niching Chimp Optimization Algorithm (RN-ChOA) from Bo et al., (2022). Chaotic JAYA (CJAYA4) from Premkumar (2021). Weighted mean of vectors optimization algorithm (INFO) from Demirtas and Koc, (2022).

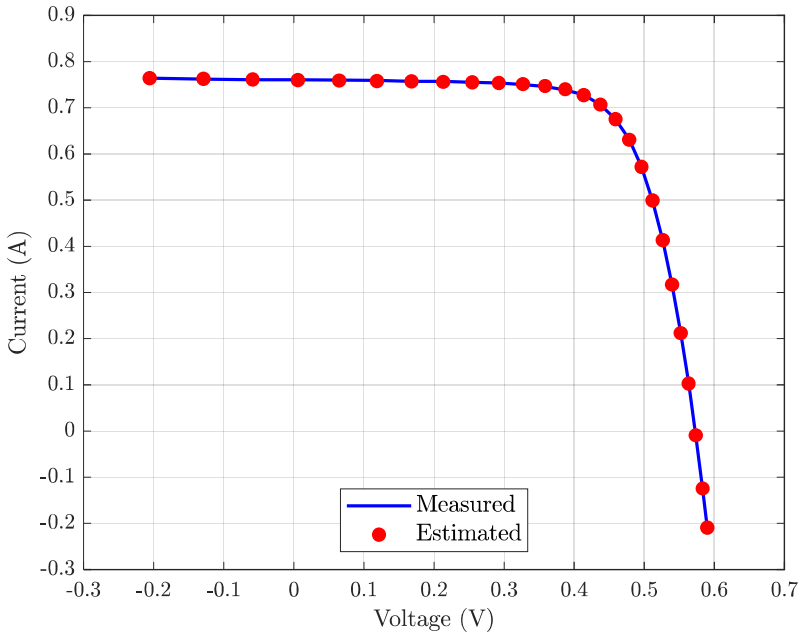

Figure 6 – Measured and estimated data: $I - V$ curve.

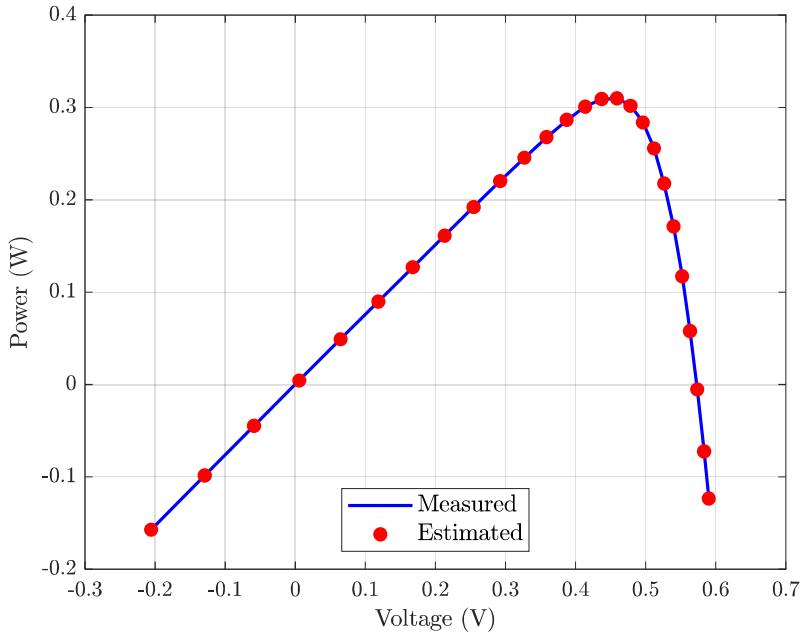

Figure 7 – Measured and estimated data: $P - V$ curve.

The Swarm MVMO proved to be an efficient algorithm in estimating the parameters of the DDM reaching the same RSME values in the literature. However, its behavior along each iteration may vary, as shown in Fig. 5 where we can see the RMSE values per run. Although DDM achieved low RMSE values, this model had a large oscillation that is attributed to the large number of parameters to be estimated and the nature of the Swarm MVMO algorithm that generates the initial population randomly within the limits established for each parameter. Similar behavior can be seen in Demirtas and Koc, (2022) and Premkumar et al., (2021).

Table 3 – Comparison between measured and estimated data.

Item	V_{mea} (V)	I_{mea} (A)	I_{est} (A)	$\|I_{ae}\|$ (A)	P_{mea} (W)	P_{est} (W)	$\|P_{ae}\|$ (W)
1	-0.2057	0.7640	**0.7641**	0.0001	-0.1572	**-0.1572**	0.0000
2	-0.1291	0.7620	**0.7627**	0.0007	-0.0984	**-0.0985**	0.0001
3	-0.0588	0.7605	**0.7614**	0.0009	-0.0447	**-0.0448**	0.0001
4	0.0057	0.7605	**0.7602**	0.0003	0.0043	**0.0043**	0.0000
5	0.0646	0.7600	**0.7591**	0.0009	0.0491	**0.0490**	0.0001
6	0.1185	0.7590	**0.7581**	0.0009	0.0899	**0.0898**	0.0001
7	0.1678	0.7570	**0.7571**	0.0001	0.1270	**0.1270**	0.0000
8	0.2132	0.7570	**0.7562**	0.0008	0.1614	**0.1612**	0.0002
9	0.2545	0.7555	**0.7551**	0.0004	0.1923	**0.1922**	0.0001
10	0.2924	0.7540	**0.7537**	0.0003	0.2205	**0.2204**	0.0001
11	0.3269	0.7505	**0.7514**	0.0009	0.2453	**0.2456**	0.0003
12	0.3585	0.7465	**0.7474**	0.0009	0.2676	**0.2679**	0.0003
13	0.3873	0.7385	**0.7401**	0.0016	0.2860	**0.2866**	0.0006
14	0.4137	0.7280	**0.7274**	0.0006	0.3012	**0.3009**	0.0002
15	0.4373	0.7065	**0.7070**	0.0005	0.3090	**0.3092**	0.0002
16	0.4590	0.6755	**0.6753**	0.0002	0.3101	**0.3100**	0.0001
17	0.4784	0.6320	**0.6309**	0.0011	0.3023	**0.3018**	0.0005
18	0.4960	0.5730	**0.5721**	0.0009	0.2842	**0.2838**	0.0005
19	0.5119	0.4990	**0.4995**	0.0005	0.2554	**0.2557**	0.0003
20	0.5265	0.4130	**0.4135**	0.0005	0.2174	**0.2177**	0.0003
21	0.5398	0.3165	**0.3172**	0.0007	0.1708	**0.1712**	0.0004
22	0.5521	0.2120	**0.2121**	0.0001	0.1170	**0.1171**	0.0001
23	0.5633	0.1035	**0.1027**	0.0008	0.0583	**0.0579**	0.0004
24	0.5736	-0.0100	**-0.0092**	0.0008	-0.0057	**-0.0053**	0.0004
25	0.5833	-0.1230	**-0.1244**	0.0014	-0.0717	**-0.0725**	0.0008
26	0.5900	-0.2100	**-0.2092**	0.0008	-0.1239	**-0.1234**	0.0005
Sum of absolute error				0.0177			0.0067
RMSE				0.0008			0.003

5. CONCLUSION

Swarm MVMO proved to be adequate and effective for estimating DDM photovoltaic parameters, presenting an RMSE of 0.986E-03, a value close to those found in the literature. This low error allowed the parameters obtained in Swarm MVMO to achieve a good fit in the *I-V* and *P-V* curves between the measured and estimated data. Although the Swarm MVMO method presents good results adequacy in estimation processes, as it is a heuristic and non-deterministic method, with each new simulation, different values are calculated for the parameters, although limited between the maximum and minimum values, which generates different values of RMSE. In future work, the non-linear method will be applied together with Swarm MVMO so that it is possible to refine the parameter estimation results.

REFERENCES

Aghaei, M., Fairbrother, A., Gok, A., Ahmad, S., Kazim, S., Lobato, K., Oreski, G., Reinders, A., Schmitz, J., Theelen, M., 2022. Review of degradation and failure phenomena in photovoltaic modules, Renewable and Sustainable Energy Reviews, vol. 159, pp. 112160.

Bo, Q., Cheng, W., Khishe, M., Mohammadi, M., Mohammed, A. H., 2022. Solar photovoltaic model parameter identification using robust niching chimp optimization, Solar Energy, vol. 239, pp. 179-197.

Ćalasan, M., Aleem, S. H. E. A., Zobaa, A. F., 2021. A new approach for parameters estimation of double and triple diode models of photovoltaic cells based on iterative Lambert W function, Solar Energy, vol. 218, pp. 392-412.

Demirtas, M., Koc, K., 2022. Parameter extraction of photovoltaic cells and modules by info algorithm, IEEE Access, vol. 10, pp. 87022-87052.

Diab, A. A. Z., Sultan, H. M., Aljendy, R., Al-sumaiti, A. S., Shoyama, M., Ali, Z. M., 2020. Tree growth-based optimization algorithm for parameter extraction of different models of photovoltaic cells and modules, IEEE Access, vol. 8, pp. 119668-119687.

Easwarakhanthan, T., Bottin, J., Bouhouch, I., Boutrit, C., 1986. Nonlinear minimization algorithm for determining the solar cell parameters with microcomputers. International Journal of Solar Energy, vol. 4, n. 1, p. 1-12.

Elhammoudy, A., Elyaqouti, M., Hmamou, D. B., Arjdal, E. H., Saadaoui, D., Lidaighbi, S., Choulli, I., 2023. A novel numerical method for estimation the photovoltaic cells/modules parameters based on dichotomy method, Results in Optics, vol. 12, pp. 100445.

Elkholy, A., El-ela, A. A. A., 2019. Optimal parameters estimation and modeling of photovoltaic modules using analytical method, Heliyon, vol. 5, n. 7, pp. 02137.

Erlich, I., Venayagamoorthy, G. K., Worawat, N., 2010. A mean-variance optimization algorithm, IEEE Congress on Evolutionary Computation, Barcelona, Spain, 2010, pp. 1-6.

Gao, S., Wang, K., Tao, S., Jin, T., Dai, H., Cheng, J., 2021. A state-of-the-art differential evolution algorithm for parameter estimation of solar photovoltaic models, Energy Conversion and Management, vol. 230, pp. 113784.

Gao, X., Cui, Y., Hu, J., Xu, G., Yu, Y., 2016. Lambert W-function based exact representation for double diode model of solar cells: comparison on fitness and parameter extraction, Energy Conversion and Management, vol. 127, pp. 443-460.

Huynh, D. C., Dunnigan, M. W., Barbalata, C., 2022. Estimation for model parameters and maximum power points of photovoltaic modules using stochastic fractal search algorithms, IEEE Access, vol. 10, pp. 104408-104428.

Long, W., Jiao, J., Liang, X., Xu, M., Tang, M., Cai, S., 2022. Parameters estimation of photovoltaic models using a novel hybrid seagull optimization algorithm, Energy, vol. 249, pp. 123760.

Nguyen, T. T., Nguyen, T. T., Tran, T. N., 2022. Parameter estimation of photovoltaic cell and module models relied on metaheuristic algorithms including artificial ecosystem optimization, Neural Computing and Applications, vol. 34, n. 15, pp. 12819-12844.

Oliva, D., Aziz, M. A. E., Hassanien, A. E., 2017. Parameter estimation of photovoltaic cells using an improved chaotic whale optimization algorithm, Applied Energy, vol. 200, pp. 141-154.

Premkumar, M., Jangir, P., Sowmya, R., Elavarasan, R. M., Kumar, B. S., 2021. Enhanced chaotic JAYA algorithm for parameter estimation of photovoltaic cell/modules, Isa Transactions, vol. 0, pp. 139-166.

Ramadan, H. A., Khan, B., Diab, A. A. Z., 2022. Accurate parameters estimation of three diode model of photovoltaic modules using hunter–prey and wild horse optimizers, IEEE Access, vol. 10, pp. 87435-87453.

Ramadan, A., Kamel, S., Hassan, M. H., Ahmed, E. M., Hasanien, H. M., 2022. Accurate Photovoltaic Models Based on an Adaptive Opposition Artificial Hummingbird Algorithm, Electronics, vol. 11, n. 3, pp. 318.

Ridha, H. M., Hizam, H., Gomes, C., Heidari, A. A., Chen, H., Ahmadipour, M., Muhsen, D. H., Alghrairi, M., 2021. Parameters extraction of three diode photovoltaic models using boosted LSHADE algorithm and Newton Raphson method, Energy, vol. 224, pp. 120136.

Ridha, H. M., Hizam, H., Mirjalili, S., Othman, M. L., Ya'acob, M. E., Abualigah, L., 2022. A novel theoretical and practical methodology for extracting the parameters of the single and double diode photovoltaic models, IEEE Access, vol. 10, pp. 11110-11137.

Rueda, J. L., Erlich, I., 2013a. Evaluation of the mean-variance mapping optimization for solving multimodal problems, 2013 IEEE Symposium on Swarm Intelligence, pp. 1-8.

Rueda, J. L., Erlich, I., 2013b. Hybrid mean-variance mapping optimization for solving the IEEE-CEC 2013 competition problems, 2013 IEEE Congress on Evolutionary Computation, pp. 1-8.

Saadaoui, D., Elyaqouti, M., Assalaou, K., Hmamou, D. B., Lidaighbi, S., 2021. Parameters optimization of solar PV cell/module using genetic algorithm based on non-uniform mutation, Energy Conversion and Management, vol. 12, pp. 100129.

Sharadga, H., Hajimirza, S., Cari, E. P. T., 2021. A fast and accurate single-diode model for photovoltaic design, IEEE Journal of Emerging and Selected Topics in Power Electronics, vol. 9, n. 3, pp. 3030-3043.

Shouman, N., Hegazy, Y. G., Omran, W. A., 2021. Hybrid mean-variance mapping optimization algorithm for solving stochastic based dynamic economic dispatch incorporating wind power uncertainty, Electric Power Components and Systems, pp. 1-16.

Yaghoubi, M., Eslami, M., Noroozi, M., Mohammadi, H., Kamari, O., Palani, S., 2022. Modified salp swarm optimization for parameter estimation of solar PV models, IEEE Access, vol. 10, pp. 110181-110194.

Yu, Y., Wang, K., Zhang, T., Wang, Y., Peng, C., Gao, S., 2022. A population diversity-controlled differential evolution for parameter estimation of solar photovoltaic models, Sustainable Energy Technologies and Assessments, vol. 51, pp. 101938.